Towards an Excitable Microwave Spike Generator for Future Neuromorphic Computing

Qusay Al-Taai[*#1], Razvan Morariu[#1], Jue Wang[#1], Abdullah Al-Khalidi[#1], Ali Al-Moathin[#1], Bruno Romeira[#2], José Figueiredo[#3] and Edward Wasige[#1]

[1]High Frequency Electronics Group, James Watt School of Engineering, University of Glasgow, UK

[2]International Iberian Nanotechnology Laboratory, Portugal

[3]Centra-Ciências and Departamento de Física, Faculdade de Ciências, Universidade de Lisboa, Campo Grande, 1749-016 Lisboa, Portugal

* qusayraghibali.al-taai@glasgow.ac.uk

Abstract — **This paper describes the systematic approach to develop low power consumption excitable neuromorphic spike generators using nano-sized resonant tunnelling diode (RTD), including fabrication, characterization and device modelling and spike circuit simulation. The fabrication process of nano sized RTDs has been developed and devices exhibit peak currents of up to 100 μA. The energy efficiency of the RTD spike generator can reach as low as 0.09 fJ per spike. An accurate small signal model of nano RTD has also been developed and is described. This nano-RTD technology could underpin the development of energy efficient neuromorphic computing in the very near future.**

***Keywords* — Resonant tunnelling diode, RTD, neuromorphics, ultrafast electronics, spike generator.**

I. Introduction

The recent rise of Artificial Intelligence (AI) systems powered by computers that can learn without the need for explicit instructions is transforming our digital economy and our society as a whole. Computational deep neural network models are inspired by information processing in the human brain. However, today's computing hardware, based on von Neumann architectures, is inefficient at implementing these neural networks largely because of the high power consumption per unit area required, typically >10 W/cm^2 compared to around 0.01 W/cm^2 for the human brain [1]. As such, research for new low energy computing paradigms is underway.

The nanometre-sized RTD (nano-RTD) is a nanoelectronic structure that can be easily integrated with a photodiode on a chip working at room temperature. Its unique current-voltage characteristic exhibits a negative differential resistance (NDR) region, and so it can be used in the design of excitable spike (pulsed) generators to produce short electrical and optical pulses mimicking the spiking behaviour of biological neurons thus making it one of the target candidates for such neuromorphic applications [2]. RTD has attracted a lot of research interest for terahertz (THz) [3] and logic applications [4], but here we propose a novel application in neuromorphic computing.

In this paper, we report on the systematic approach to develop low power consumption RTD technology, including device fabrication, characterization, accurate device modelling process and spike generator circuit simulation. The results are expected to pave the way for building low power consumption excitable electrical spike generators operating in the microwave frequency range and aimed at the currently fast evolving neuromorphic computing applications.

II. Device Design and Fabrication

A. Epitaxial structure design

In this section we describe the design of the epitaxial RTD wafers. It was grown on a semi-insulating InP substrate by molecular beam epitaxy (MBE). The double barrier quantum well (DBQW) structure of RTD comprises a 5.7 nm $In_{0.53}Ga_{0.47}As$ quantum well, 1.7 nm AlAs barriers, with 100 nm thick lightly doped InAlGaAs spacers. The collector and emitter layers are made of highly Si doped $In_{0.53}Ga_{0.47}As$ layers.

Details of the epitaxial layer structure are shown in Table 1.

Table 1. Structure Specification of 1000A wafer.

Layer	Type	Doping level	Material	Thickness (Å)	Description
12	N++	2.0e19	InGaAs	1000	Contact
11	N+	2.0e18	InAlAs	1000	Collector
10	N-	2.0e16	InAlGaAs	1000	Spacer
9	I	---	InGaAs	20	---
8	I	---	AlAs	17	Barrier
7	I	---	InGaAs	57	Well
6	I	---	AlAs	17	Barrier
5	I	---	InGaAs	20	---
4	N-	2.0e16	InGaAs	200	Spacer
3	N+	2.0e18	InAlAs	1000	Emitter
2	N++	2.0e19	InGaAs	5000	Contact
1	I	---	In(x)AlAs	1000	---
Substrate			InP		

B. Design and Fabrication process

We designed and fabricated mesa structures with circular geometry with diameters of 500, 700, 800 nm. The fabrication process starts with metal evaporation of Ti/Pd/Au to form the top contact of the RTD. Dry etching InGaAs with $Cl_2/CH_4/H_2$ gases at 60˚C to define the RTD mesa. The bottom contact metal (Ti/Pd/Au) was then evaporated. Low dielectric constant polymer Benzocyclobutene (BCB) was used for device

passivation, followed by an etch back process. Finally, bond-pad metallisation was carried out using Ti/Au. Fig.1 shows the SEM images for different stages of nano-RTD fabricated devices.

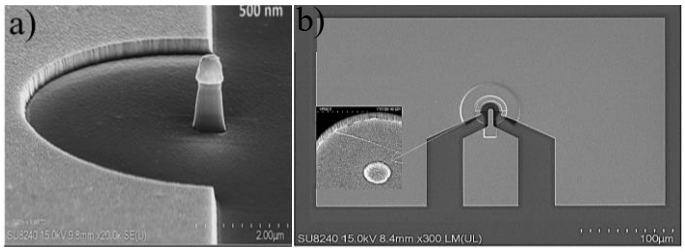

Fig. 1. SEM images of a fabricated 500 nm RTD a) top contact/mesa and bottom contact, and b) the bond pads of completed device; the inset showing the bond pad over the 500 nm top contact.

III. Measurements and Results

A. Static current-voltage (I-V) characterization of RTDs

The I-V characterisation of the fabricated devices was done using the Keysight's semiconductor parameter analyser (B1500). The measured characteristics of the fabricated nano-RTD devices with diameters of 500, 700, and 800 nm are shown in Fig. 2. The peak DC power consumption of 500 nm RTD is 64.8 μW. For the 500 nm diameter device, the energy consumption per cycle can reach as low as 0.09 fJ if it is employed in an oscillatory circuit.

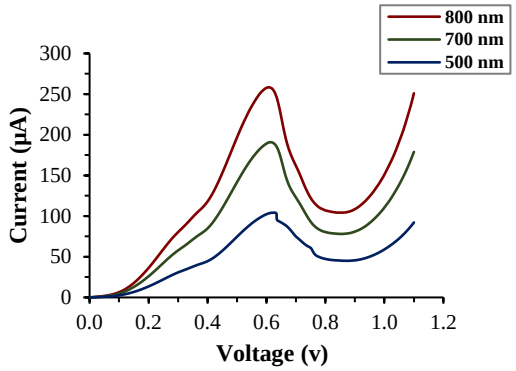

Fig. 2. I-V characteristics of 500, 700 & 800 nm RTD device.

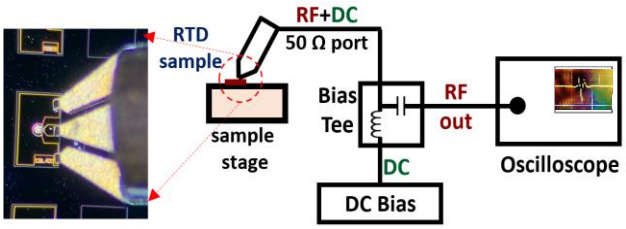

Fig.3, Schematic circuit for the self-oscillation measurement.

To assess the spiking behaviour of the devices, an RTD device of 500 nm mesa was used. Fig.3. shows the setup for this measurement. While Fig.4 shows the measurement equivalent circuit. Here, R_b/L_b represent the resistance and inductance of the biasing cable. $L_{bias\text{-}tee}$ and $C_{bias\text{-}tee}$ denote the inductance and capacitance of the bias-tee while R_L represent the input impedance of the oscilloscope.

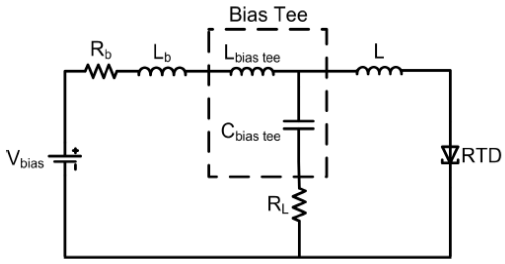

Fig. 4. The measurement equivalent circuit of self-oscillation measurement.

Relaxation oscillations were observed on the oscilloscope. When the RTD was biased at 0.6 V in the NDR region near the peak voltage, Vp, the time domain pulse was shown in Fig. 5. The number of spikes can be controlled by adjusting the applied biasing voltage. It is worth to note that phase of the spike is opposite depending on the bias position. The results are consistent with our simulation presented in section D.

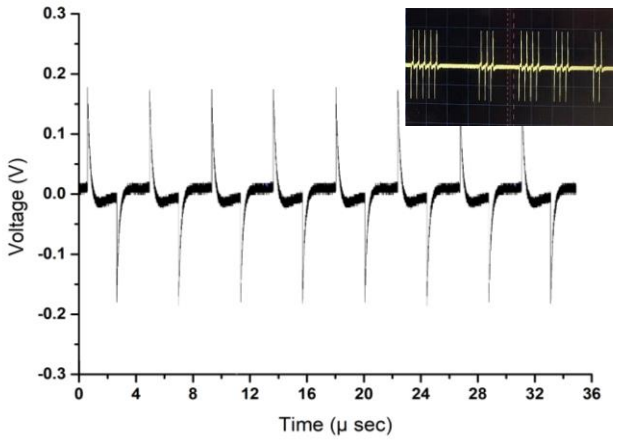

Fig. 5. Experimental traces of output spikes generated by 500 nm nano-RTD device when biasing around peak point. The inset presents the number of spikes during simply adjustment of biasing voltage.

Fig.6 shows another set of experimental results of generated spikes using an RTD-oscillator [5]. The oscillator was driven by pseudo-random bit sequence (PRBS) with an amplitude of 1V, biased at -0.59 V close to peak voltage V_p, and the frequency of the PRBS was set at 500 MHz. The resultant spiking behaviour is shown in Fig.7. The amplitude of the spikes is around 2.5 mV, and the spike duration is 450 psec. The amplitude of spikes is rather low (~2mV), which is attenuated due to the shunt circuit of the RTD-oscillator circuit. In this experiment, we find that when applying an electrical signal and biasing the RTD in either first or second PDR regions slightly below/above the peak/valley voltage, we found that the RTD responds to the external signal and generate spikes; only if the PRBS signal exceeds a threshold point, which mainly depends on the biasing value. Two main factors characterise spiking behaviour namely the biasing positions and the amplitude of PRBS input signal. In addition, the control of the pulse shape can be achieved via several parameters, such as the adjusting between time constants associated to the capacitive part of the circuit (RC time) and the inductive part (inductance associated time constant).

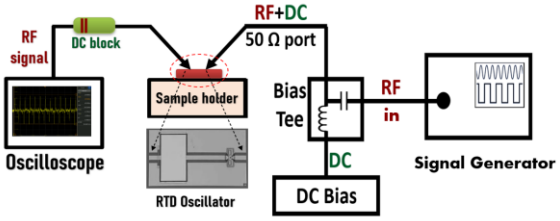

Fig.6, Schematic circuit for the spike measurements.

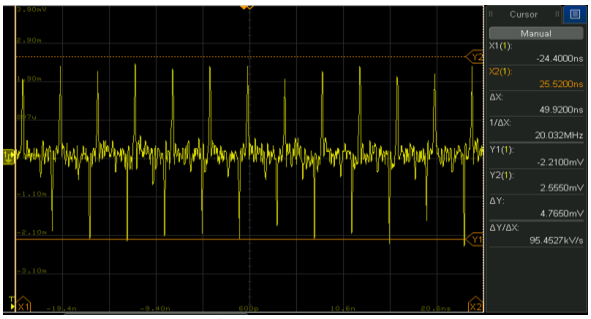

Fig. 7. Experimental traces of output spikes generated by an RTD driven by pulse generator. The input bias voltage the PRBS square wave amplitude was set to 1V, the RTD oscillator was biased at 0.56V, the frequency was set at 500 MHz.

B. High frequency characterisation of nano-RTDs

Here, a vector network analyzer (VNA) was used. The calibration of the VNA was done using the short-open-load-through (SOLT) technique with a port power of −17 dBm. The frequency range was 10 MHz–110 GHz. Fig. 8. shows the measured S-parameters (for a bias point in the NDR region) of 500 nm RTD which reflect the stability of nano RTD devices.

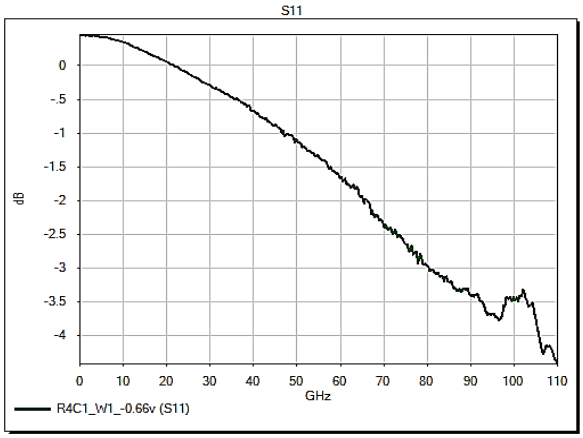

Fig. 8. S-parameters (S11) of 500 nm RTD device.

C. Small-signal modelling of nano RTD devices

The small signal equivalent circuit model of the RTD, first introduced in [6] consists of the metal-semiconductor contact and access resistance R_s, in series with the parallel combination of the device self-capacitance C_n together with the device conductance G_n which models the device current–voltage characteristics, and the quantum well inductance L_{qw}, which models the charging and discharging effects of the quantum well [7]. The complete device circuit, shown in Fig. 9, is completed by the extrinsic elements C_p and L_p, which model the parasitic components introduced by the metallic bond-pads [8].

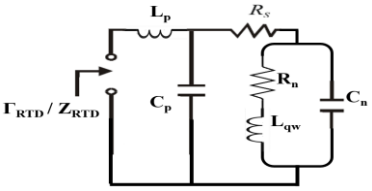

Fig. 9. Small-signal equivalent circuit of an RTD device comprises R_s R_n, L_{qw} and C_n. The bond-pad is modelled by parasitic elements L_p and C_p.

In order to accurately determine the realised device equivalent circuit elements, the acquired S-parameter data was first converted to real and imaginary Z-parameters and fitted using the proposed model over the entire frequency range using a direct optimization procedure [9].

Good agreement between measurement and simulation was obtained across the entire nano RTD device bias range for frequencies up to 110 GHz. This is illustrated by the graphs in Fig. 10, with only two bias points results are shown, i.e. 0.4V in 1st PDR region and 0.65V in NDR region.

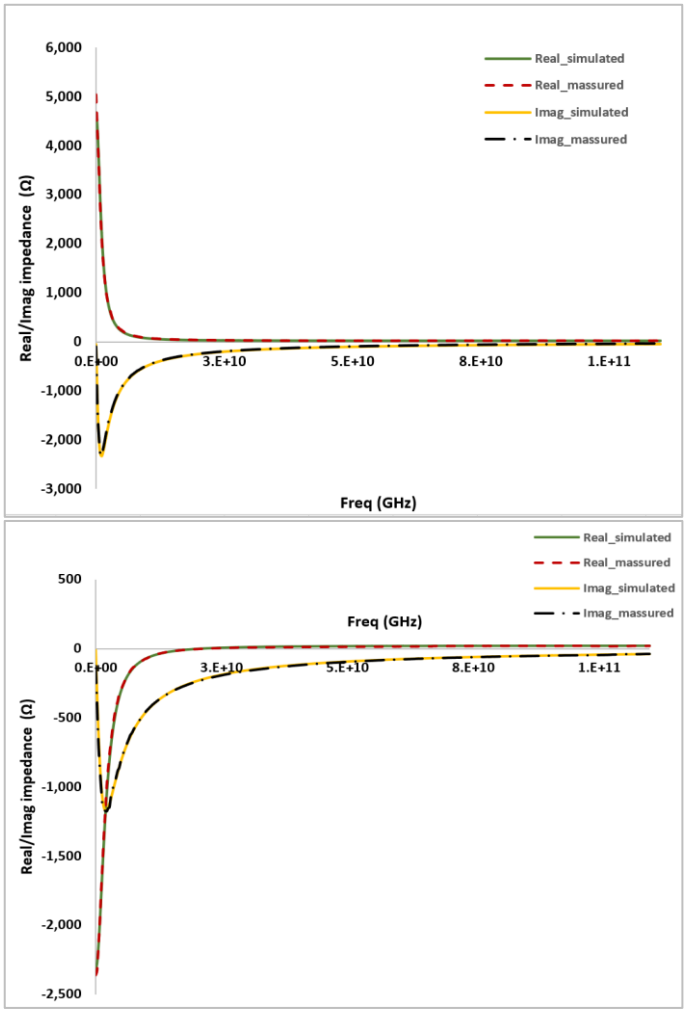

Fig. 10. Graphs of real and imaginary parts of Z-parameters, the dashed lines are for measured while the sold lines for simulated parameters for a 500 nm diameter nano-RTD in the NDR region at a) 0.4V and b) 0.65V.

A summary of the extracted frequency independent RTD parameters corresponding to the three regions of interest is given in Table 2.

Table 2. Summary of parameter extraction

Bias (V)	L_p (pH)	C_p (fF)	R_s (Ω)	G_n (mΩ^{-1})	C_n (fF)	L_{qw} (nH)
0.4	9.35	0.1	22	0.639	33.3	2
0.65	9.35	0.1	22	-1.563	33	-2.2
1	9.35	0.1	22	0.505	33.7	2.7

As predicted by the measured device DC characteristics, the differential conductance G_n becomes negative in the NDR region, with its relatively low magnitude attributed to the designed sub-micron device active area. Furthermore, a bias dependency of the device self-capacitance was observed, with a peak value obtained within the NDR region. This observation is consistent with the predicted behaviour described in [10], and is attributed to the quantum capacitance component, which models the charge variation through the double-barrier quantum-well structure.

D. Relaxation and sinusoidal nanopillar RTD oscillators

Using the measured device characteristics and extracted device self-capacitances, preliminary RTD oscillator simulations have been carried out and show that nano-sized RTDs can support both relaxation and sinusoidal oscillations. Fig. 11 shows simulation oscillator results of a 500 nm diameter RTD resonated with a 34 nH inductor and driving a 700-Ω load, while Fig. 12 shows similar results for 100 pH resonating inductance. In the former case, relaxation or switching oscillations are the result while in the latter case, sinusoidal oscillations occur. Through the careful design and driving of the relaxation oscillator, an excitable pulse generator required for neuromorphic computing could be realised.

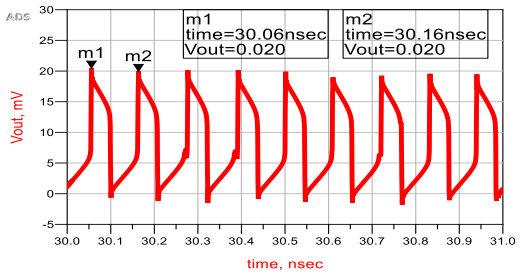

Fig. 11 Simulated relaxation oscillations with a 500 nm diameter RTD device showing that 10 GHz switching oscillations can be achieved. The resonating inductance was 34 nH.

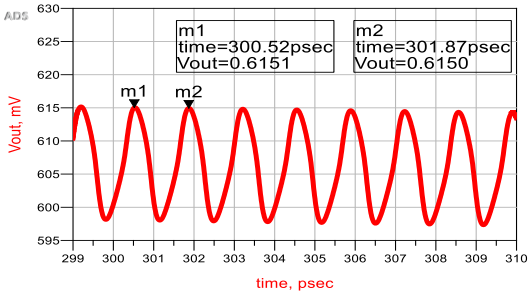

Fig. 12 Simulated sinusoidal oscillations with a 500 nm diameter RTD device showing that terahertz frequencies can be generate. The resonating inductance here was 100 pH.

CONCLUSION

The fabrication and characterization of nano-RTD devices has been described in this paper. In addition, an accurate small signal model of the device has also been described. The devices have been used in experimental demonstration of relation oscillators and in simulated sinusoidal oscillators. The power consumption can be as low as 0.09fJ per cycle. The RTD which includes a light absorption layer, can be optically controlled. This would extend our research into the optical domain. Further work in this regard is ongoing.

ACKNOWLEDGMENT

The authors would like to thank the staff of James Watt Nanofabrication Centre (JWNC) for assistance in device fabrication. The work was funded by the Horizon 2020 FET-OPEN ChipAI project, grant agreement 828841.

REFERENCES

1. Merolla, P.A., et al., *A million spiking-neuron integrated circuit with a scalable communication network and interface.* Science, 2014. **345**(6197): p. 668-673.
2. Romeira, B., et al., *Excitability and optical pulse generation in semiconductor lasers driven by resonant tunneling diode photo-detectors.* Optics Express, 2013. **21**(18): p. 20931-20940.
3. Suzuki, S., et al., *High-Power Operation of Terahertz Oscillators With Resonant Tunneling Diodes Using Impedance-Matched Antennas and Array Configuration.* IEEE Journal of Selected Topics in Quantum Electronics, 2013. **19**(1): p. 8500108-8500108.
4. Arzi, K., et al., *Subharmonic Injection Locking for Phase and Frequency Control of RTD-Based THz Oscillator.* IEEE Transactions on Terahertz Science and Technology, 2020. **10**(2): p. 221-224.
5. Wang, J., Wang, l., Li, C., Patarata Romeira, B.M., Wasige, E., *28 GHz MMIC resonant tunnelling diode oscillator of around 1mW output power.* Electronics Letters, 2013. **49**: p. 3.
6. Brown, E.R., C.D. Parker, and T.C.L.G. Sollner, *Effect of quasibound-state lifetime on the oscillation power of resonant tunneling diodes.* Applied Physics Letters, 1989. **54**(10): p. 934-936.
7. Lake, R. and Y. Junjie, *A physics based model for the RTD quantum capacitance.* IEEE Transactions on Electron Devices, 2003. **50**(3): p. 785-789.
8. Wang, J., et al. *High performance resonant tunneling diode oscillators as terahertz sources*. in *2016 46th European Microwave Conference (EuMC)*. 2016.
9. Morariu, R., et al., *Accurate Small-Signal Equivalent Circuit Modeling of Resonant Tunneling Diodes to 110 GHz.* IEEE Transactions on Microwave Theory and Techniques, 2019. **67**(11): p. 4332-4340.
10. Lake, R. and J. Yang, *A physics based model for the RTD quantum capacitance.* IEEE Transactions on Electron Devices, 2003. **50**(3): p. 785-789.